

THE EFFECT OF DEFECT FORMATION IN THE CRYSTAL LATTICE ON THE ELECTRONIC STRUCTURE AND DIELECTRIC PROPERTIES OF GaSe < Tl > SINGLE CRYSTALS SUBJECTED TO γ -IRRADIATION

S.N. MUSTAFAEVA, S.S. GUSEINOVA, M.M. ASADOV*

Institute of Physics, Azerbaijan National Academy of Sciences, Baku, AZ-1143

**Institute of Catalysis and Inorganic Chemistry, Azerbaijan National Academy of Sciences, Baku, AZ-1143*

email: solmust@gmail.com

The effect of defect formation in the crystal lattice of gallium monoselenide (GaSe) on the electronic structure was studied using density functional theory (DFT) calculations. The atomic structure of a 32-atom gallium monoselenide supercell containing both gallium vacancy and selenium vacancy is constructed. The crystal hexagonal structure of ϵ – GaSe is optimized and the lattice parameters are calculated. The band structure of a 32-atom ϵ – GaSe supercell has been studied by the DFT/LDA method (local density approximation). The atomic structure of a 32-atom gallium monoselenide supercell containing selenium vacancy has been constructed. The length of the chemical bond between atoms in different supercell configurations has been calculated.

Dielectric measurements of γ -irradiated p-type ϵ – GaSe < Tl > single crystal in the frequency range $f = 5 \cdot 10^4 - 3.5 \cdot 10^7$ Hz made it possible to establish the relaxation nature of the permittivity dispersion, as well as the nature of dielectric losses in the single crystal. The values of the static permittivity of a ϵ – GaSe < Tl > single crystal are calculated for various doses of γ -irradiation, as well as the frequency and time of relaxation. It has been established that with an increase in the γ -irradiation dose up to 2.05 Mrad, the dielectric coefficients and conductivity of the ϵ – GaSe < Tl > single crystal decrease.

Keywords: DFT/LDA calculations, supercell GaSe, single crystal, doping, γ -irradiation, complex dielectric permittivity, frequency dispersion, dielectric loss, conductivity.

PACS: 61.72.-y; 71.15.-m; 71.15.Mb; 71.20.Nr; 72.20.-i.

1. INTRODUCTION

The study of compounds of the GaX type (X – S, Se, Te) is relevant for both micro- and nanoelectronics. These monochalcogenides belong to the class of semiconductor layered compounds of the A^{III}B^{VI} type. They are important for use as active materials in various photosensitive structures, transducers, radiation detectors, light modulators, and information storage devices [1–9].

One of the III–VI type compounds is gallium monoselenide GaSe. Four polytypes of GaSe are known: β , ϵ , γ , δ modifications [6]. In particular, solar cells, efficient photodiodes, and devices for generating and detecting radiation have been created based on GaSe. The GaSe compound is easy to process and can be given the desired configuration due to strong in-plane bonding between atoms and weak interlayer van der Waals bonding. However, the mechanical properties of GaSe are poor and it has a low hardness. To improve the mechanical properties of GaSe and preserve its optical characteristics, the latter is doped with various impurities. The study of the electrical properties of semiconductors in direct and alternating electric fields provides information on the nature of charge transfer and localization of states in the band gap. In this case, it is necessary to know the temperature and frequency dependences of direct and AC conductivity.

The electrical properties of GaSe crystals are significantly affected by defect formation, the effect of external radiation, and the concentration and type of introduced impurities. For example, the introduction of tin into the crystal lattice of ϵ – GaSe results in the

compensation of acceptor levels, whose concentration in GaSe reaches 10^{17} – 10^{18} cm⁻³ [10]. The results of studying of the temperature dependence of the ohmic conductivity of p-type ϵ – GaSe single crystals doped with thallium (1, 2 and 2.5 mol.% Tl) are presented in [11]. It was found that, at temperatures $T < 250$ K, ϵ – GaSe < Tl > crystals exhibit hopping conduction with a variable hop length across their natural layers in a direct electric field. It was shown that an increase in the concentration of doping thallium in ϵ – GaSe leads to an increase in the conductivity and density of states near the Fermi level. In this case, the average distance and activation energies of hops decrease. However, the dielectric properties of ϵ – GaSe < Tl > single crystals in alternating electric fields have not yet been studied.

The purpose of this work is the ab initio studying of the effect of crystal lattice defect formation on the electronic structure of GaSe and determination of the dielectric characteristics of ϵ – GaSe < Tl > in alternating electric fields, as well as the effect of gamma irradiation on electrical properties.

2. COMPUTATIONAL AND EXPERIMENTAL METHODOLOGY

2.1 CALCULATION METHOD

Ab initio calculations were carried out in terms of density functional theory (DFT), including the electron density $\rho(\vec{r})$. It was assumed in the calculations that the energy of the ground state of the system consists of the following contributions: the kinetic energy of electrons, the energy of the Coulomb interaction of electrons, the

energy of electrons with nuclei, the exchange-correlation energy, and the energy of the external field, which includes the electron-ion single-particle energy and the constant energy of the ion-ion interaction

$$E[\rho(\vec{r})] = T_e[\rho(\vec{r})] + \int V_0(\vec{r})\rho(\vec{r}) d\vec{r} + \int \frac{\rho(\vec{r})\rho(\vec{r}')}{|\vec{r}-\vec{r}'|} d\vec{r}d\vec{r}' + E_{XC}[\rho(\vec{r})]$$

where $\int V_0(\vec{r})\rho(\vec{r}) d\vec{r}$ is the electron-nuclear interaction, $\int \frac{\rho(\vec{r})\rho(\vec{r}')}{|\vec{r}-\vec{r}'|} d\vec{r}d\vec{r}'$ is the Coulomb interaction between electrons, $E_{XC}[\rho(\vec{r})]$ is the exchange-correlation interaction, which contains all other electron-electron interactions.

The exchange-correlation functional was approximated in terms of the local density approximation (LDA). Basic principles calculations were performed using the Atomostix ToolKit program using the local density approximation. The Perdew-Zunger (PZ) exchange correlation function was used in the calculations using base sets with double zeta polarization (DZP). When optimizing the crystal structure, the maximum value of the interaction force between atoms was taken to be 0.01 eV/Å. In calculations, the maximum value of the mechanical stress tensor was assumed to be <0.01 eV/Å³ [12].

Crystal structure optimization continued until the structural parameters were balanced. Integration over the Brillouin zone was carried out at specific points using the 2 x 2 x 2 k-point according to the Monkhorst-Pack scheme. The maximum value of the kinetic energy during the wave function decomposition did not exceed 150 Ry. The wave function decomposition of valence electrons into plane waves was limited to an energy of 300 Ry. Basic principles calculations were performed for a 32-atom GaSe supercell.

2.2 EXPERIMENTAL TECHNIQUE

To conduct research, we grew thallium-doped *p*-type ε – GaSe single crystals (ε-modification, space group $P\bar{6}m2 (D_{3h}^1)$) by the Bridgman method. The content of thallium in *p*-GaSe was 0.5 mol %.

Samples for electrical measurements were fabricated in a “sandwich” structure; an alternating electric field was applied across the natural layers of a GaSe single crystal. Silver paste was used as a contact material. The thickness of the studied *p*-GaSe single crystals was 660 μm, and the subcontact area was 0.15 cm². Electrical measurements were carried out at *T* = 300 K.

The dielectric coefficients of the single crystal GaSe <Ti> were measured by the resonance method. The frequency range of the alternating electric field was $f = 5 \cdot 10^4 - 3.5 \cdot 10^7$ Hz. During electrical measurements, the samples were placed in a shielded chamber. The amplitude of the alternating electric field applied to the samples corresponded to the Ohmic region of the current-voltage characteristic. The accuracy of determining the resonant values of the capacitance and

quality factor ($Q = 1/\text{tg}\delta$) of the measuring circuit is limited by errors associated with the degree of resolution of readings by devices. The capacitor calibration had an accuracy of ± 0.1 pF. The reproducibility of the resonance position was ±0.2 pF in terms of capacitance and ±1.0–1.5 divisions of the scale in terms of quality factor ($Q = 1/\text{tg}\delta$). In this case, the largest deviations from the average values were 3–4% for ε and 7% for tgδ [7-10].

Gamma-irradiation of the samples was carried out on a continuous radiation chemical installation (RKhUND - 20000) from a source of Co⁶⁰. The energy of γ-quanta was 1.25 MeV. The dose of γ-irradiation was accumulated by successive exposures in the same sample and amounted to 50 krad and 2.05 Mrad. Dielectric measurements of the samples were carried out after each irradiation.

3. CALCULATION, EXPERIMENTAL RESULTS AND DISCUSSION

3.1 CALCULATION RESULTS

In terms of DFT theory, the LDA approximation was used for the calculation. The main shortcomings of this approach are that it is based on a one-electron description of the electron density of the system, which includes an orbital-independent potential. DFT/LDA calculation of the band structure of semiconductors usually results in an underestimated value of the band gap (E_g) in comparison with the experiment. In the LDA calculation for densities of states characteristic of solids, the determined range of exchange-correlation effects is short. DFT/LDA is better applicable to solids that are close to a homogeneous gas (for example, the free electrons of a metal). On the other hand, the advantages of DFT/LDA are that it allows to accurately describe the kinetic part of the system's Hamiltonian, the long-range part of the Coulomb interaction, and calculate the model parameters.

In order to correct the shortcomings of the DFT/LDA calculations of the band structure, known corrections are used (for example, double counting, including the Hubbard model and the Anderson impurity model) and calculation methods [Giu]. Below are the results of calculations of the electronic structure of ε – GaSe, which include the determination of the exchange-correlation potential (functional) in the LDA approximation. To eliminate the shortcomings of LDA and to more accurately calculate the exchange-correlation energy, generalized gradient expansion (GGA) is usually used. DFT/GGA calculation of electronic properties includes different ways of specifying functions. For large gradients of the density of states, these functions enable to preserve the specified properties of the system.

The results of DFT calculations of the GaSe band structure using the generalized gradient expansion (GGA) will be presented in another paper. In DFT/LDA calculations, individual layers were modeled on supercells composed of a unit cell of a layered ε – GaSe crystal (space group $P\bar{6}m2 (D_{3h}^1)$) (Fig. 1). The general view of such supercells is shown in Fig. 2a-c.

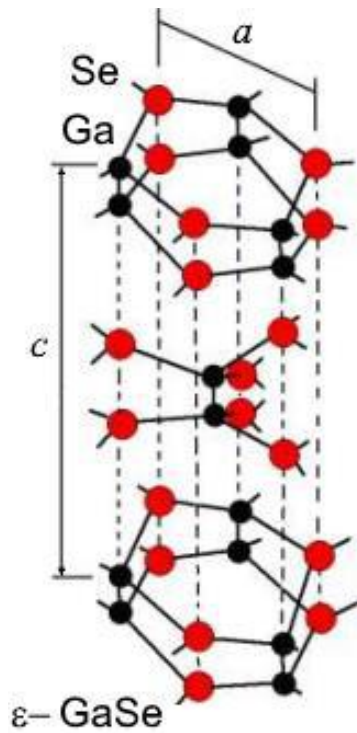
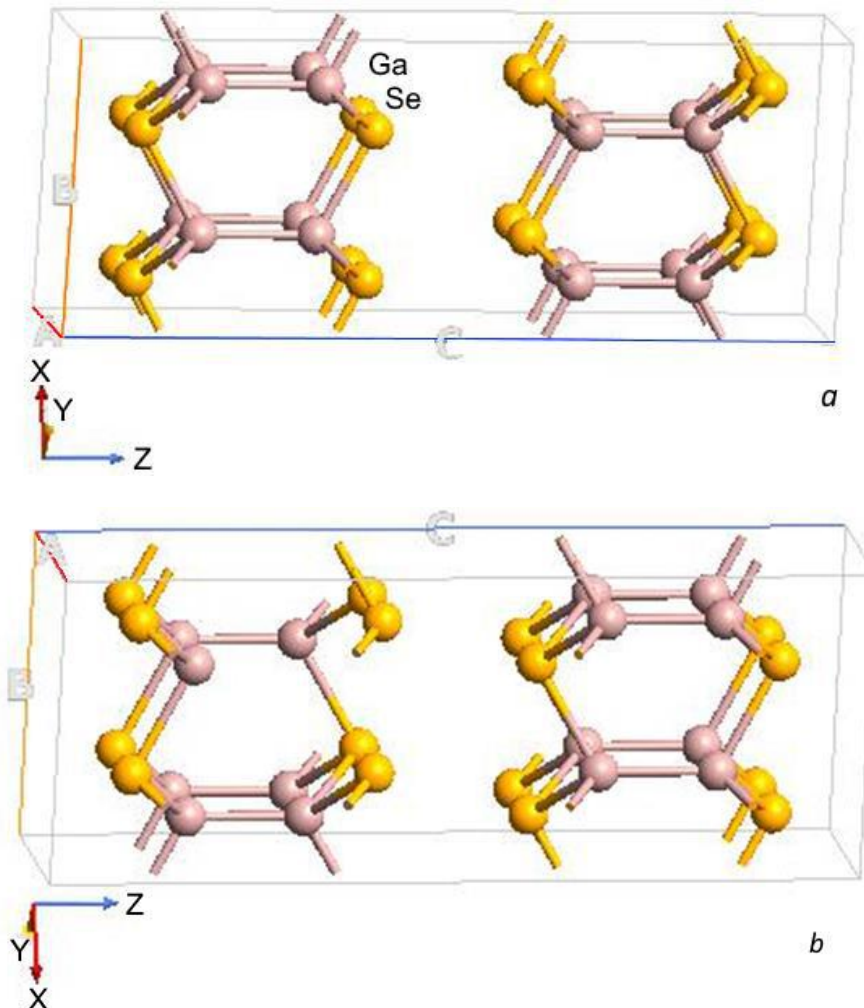


Fig. 1. Crystalline structure and layer stacking for crystal ϵ -polytype GaSe.

Comparison of the results of DFT calculations of the structural parameters of GaSe ($a = 3.706 \text{ \AA}$; $c = 15.778 \text{ \AA}$) with the lattice parameters of bulk ϵ -GaSe samples ($a = 3.755 \text{ \AA}$; $c = 15.946 \text{ \AA}$ [13]; $a = 3.755 \text{ \AA}$; $c = 15.940 \text{ \AA}$ [6]) indicates good agreement between them. The band gap (E_g) of the 32-atom $\text{Ga}_{16}\text{Se}_{16}$ supercell is $E_g = 0.99 \text{ eV}$ when calculated by the LDA method. The LDA method was also used to calculate the E_g value of the $\text{Ga}_{15}\text{Se}_{16}$ supercell containing Ga vacancy (Fig. 3a). In the case of Ga vacancy, the value of $E_g = 1.6 \text{ eV}$. The calculated E_g for $\text{Ga}_{16}\text{Se}_{15}$ supercell containing the Se vacancy is 1.7 eV (Fig. 3b). This value of E_g is also underestimated compared to the experimental data ($1.952\text{--}2.086 \text{ eV}$).

This underestimation of E_g of the ϵ -GaSe is due to a well-known shortcoming of the LDA approximation. The length of intralayer and interlayer bonds (Se-Ga, Ga-Ga and Se-Se) was calculated in a 32-atom GaSe supercell. In particular, the bond length between the 12th Se atom and the 25th Ga, the 24th and 26th Ga, the 30th Se and the 12th Se atom (Fig. 4) agrees with the experimental data. In other words, good agreement with the experimental data for ϵ -GaSe is obtained: $d(\text{Se-Ga}) = 2.485 \text{ \AA}$, $d(\text{Ga-Ga}) = 2.383 \text{ \AA}$, $d(\text{Se-Se}) = 3.840 \text{ \AA}$.



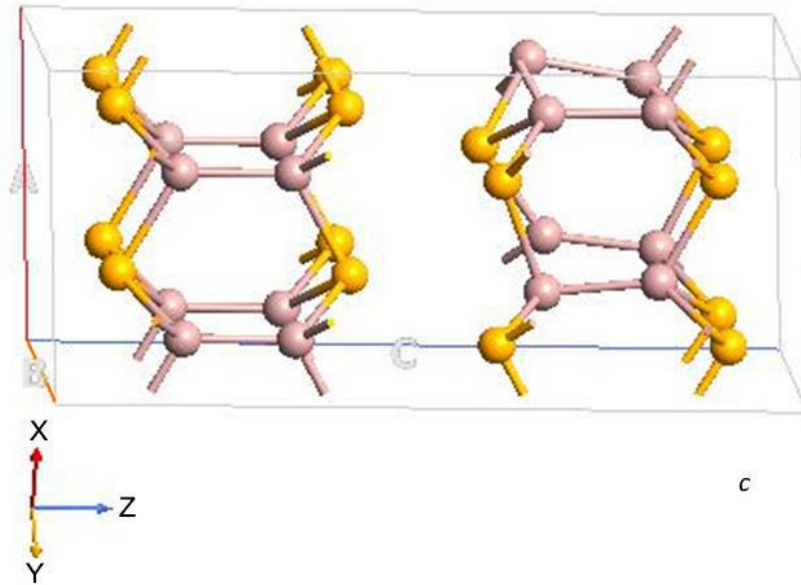


Fig. 2. Atomic structure of a gallium monoselenide supercell: *a* – 32-atom GaSe; *b* – 32-atom GaSe containing gallium vacancy; *c* – 32-atom GaSe containing selenium vacancy.

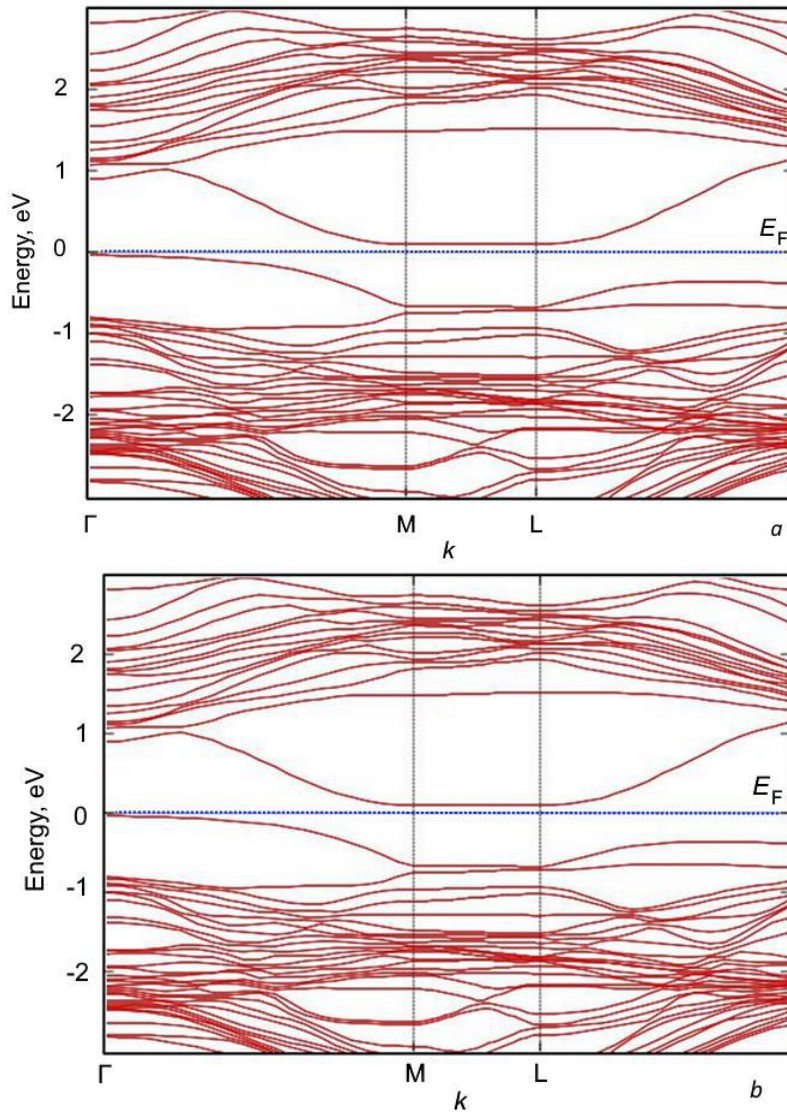


Fig. 3. Band structure of a 32-atom $\text{Ga}_{16}\text{Se}_{16}$ supercell calculated in the LDA approximation: *a* – $\text{Ga}_{15}\text{Se}_{16}$ supercell containing Ga vacancy, *b* – $\text{Ga}_{16}\text{Se}_{15}$ supercell containing Se vacancy.

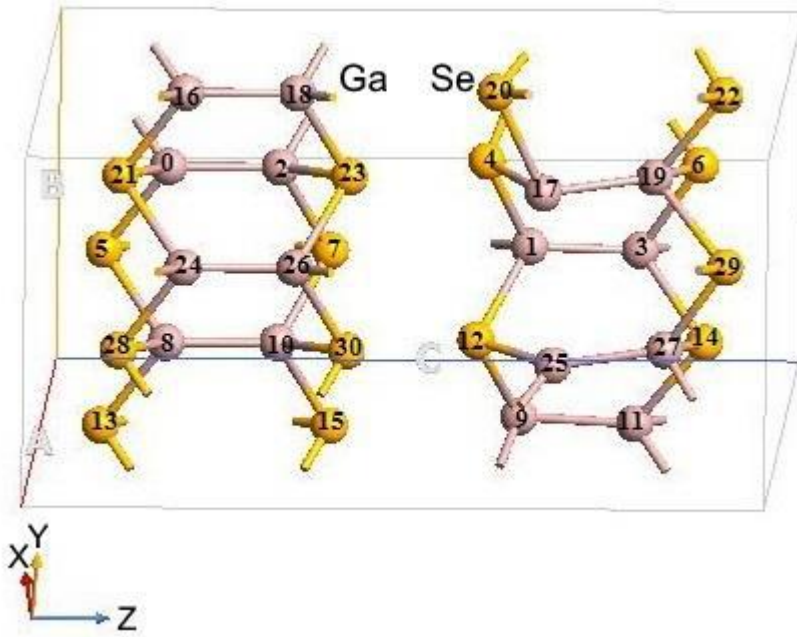


Fig. 4. Atomic structure of a 32-atom GaSe supercell containing a selenium vacancy. The numbers in the figure indicate the numbers of atoms used to calculate the chemical bond length.

3.2. EXPERIMENTAL RESULTS

Figure 5 shows the frequency dependences of the real component of the complex permittivity (ϵ') of the $\epsilon - \text{GaSe} \langle \text{Tl} \rangle$ sample before (curve 1) and after γ -irradiation with different doses (curves 2 and 3). As follows from Fig. 5 ϵ' of the unirradiated GaSe $\langle \text{Tl} \rangle$ sample undergoes significant dispersion with increasing frequency. Thus, in the studied frequency range, the value of ϵ' decreases by an order of magnitude with increasing frequency. At the same time, the main decrease in ϵ' is observed in the frequency range of $5 \times 10^4 - 10^6$ Hz, and at $f > 10^6$ Hz, ϵ' weakly depended on frequency. A similar situation was observed in the GaSe $\langle \text{Tl} \rangle$ sample after its γ -irradiation with a dose of $D_\gamma = 50$ krad. The specified irradiation

dose almost did not change the dielectric permittivity of the sample, slightly increasing its value before γ -irradiation. A higher dose of γ -irradiation (2.05 Mrad) led to a decrease in the value of ϵ' of the GaSe $\langle \text{Tl} \rangle$ sample (by a factor of 1.6 at $f = 5 \times 10^4$ Hz). The nature of the change in ϵ' with frequency indicates the relaxation dispersion of the permittivity of the GaSe $\langle \text{Tl} \rangle$ single crystal both before and after its irradiation with γ quanta. The smallest value of ϵ' measured at high frequency ($f = 3.5 \times 10^7$ Hz) can be considered as the optical permittivity (ϵ'_{opt}) of the GaSe $\langle \text{Tl} \rangle$ single crystal. The ϵ'_{opt} values of the GaSe $\langle \text{Tl} \rangle$ sample before and after γ -irradiation were approximately the same (table). Those γ -irradiation even with a dose of 2.05 Mrad almost did not change the value of ϵ'_{opt} .

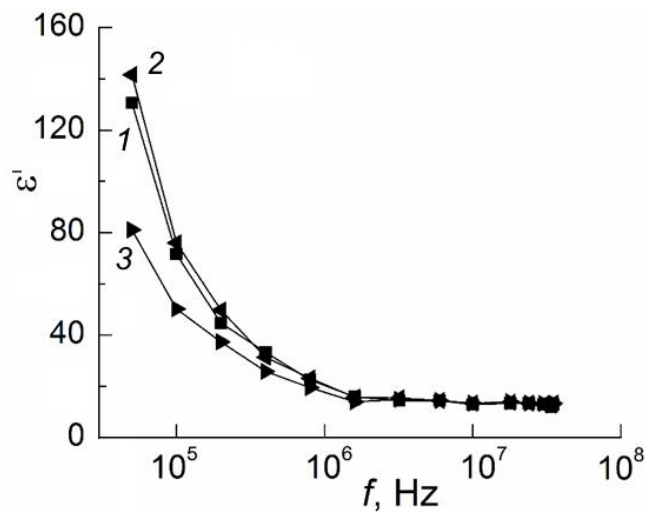


Fig. 5. Frequency dispersion of the dielectric permittivity of a single crystal p-type $\epsilon - \text{GaSe} \langle \text{Tl} \rangle$ before (curve 1) and after (curves 2 and 3) γ -irradiation with doses D_γ : 2 – 50 krad; 3 – 2.05 Mrad. $T = 300$ K.

Dielectric parameters of single crystal $\epsilon - \text{GaSe} \langle \text{Tl} \rangle$ before and after γ -irradiation

D_γ, rad	$\text{tg}\delta_{\text{max}}$	ϵ'_{opt}	ϵ'_{st}	$\Delta \epsilon'$	f_i, Hz	f_r, Hz
0	2.11	12.9	254.9	242	10^5	$2.2 \cdot 10^4$
$5 \cdot 10^4$	1.91	12.7	210	197.3	10^5	$2.5 \cdot 10^4$
$2.05 \cdot 10^6$	1.72	12.7	174.7	162	10^5	$2.7 \cdot 10^4$

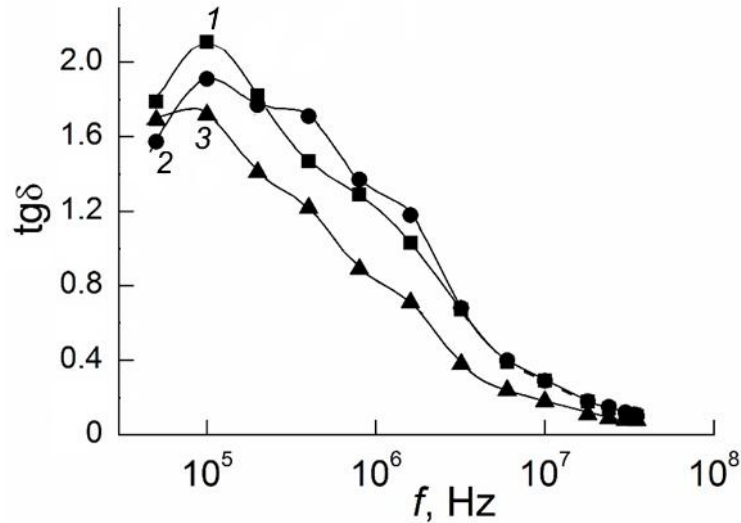


Fig. 6. Frequency dependences of the dielectric loss tangent in a single crystal p-type $\epsilon - \text{GaSe} \langle \text{Tl} \rangle$ before (curve 1) and after (curves 2 and 3) γ -irradiation with doses D_γ : 2 – 50 krad; 3 – 2.05 Mrad.

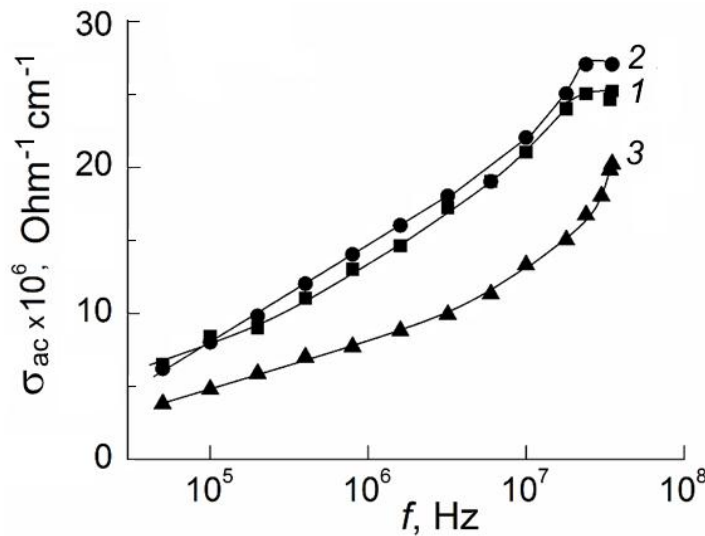


Fig. 7. Frequency-dependent ac-conductivity of a single crystal p-type $\epsilon - \text{GaSe} \langle \text{Tl} \rangle$ before (curve 1) and after (curves 2 and 3) γ -irradiation with doses D_γ : 2 – 50 krad; 3 – 2.05 Mrad.

Fig. Figure 6 shows the frequency dependences of the dielectric loss tangent ($\text{tg}\delta$) in a $\text{GaSe} \langle \text{Tl} \rangle$ single crystal before (curve 1) and after γ - irradiation (curves 2 and 3). At $f = 10^5 \text{ Hz}$, curves 1, 2, and 3 passed through a maximum and then had a decreasing character. The values of $\text{tg}\delta_{\text{max}}$ in the non-irradiated and γ -irradiated $\text{GaSe} \langle \text{Tl} \rangle$ are given in the table. From the table and Figure 6 it is seen that with an increase in the dose of γ -irradiation, the values of $\text{tg}\delta_{\text{max}}$ in the $\text{GaSe} \langle \text{Tl} \rangle$ sample decrease, and the peak itself becomes more blurred. At high frequencies ($f \geq 10^7$

Hz), the values of $\text{tg}\delta$ in the $\text{GaSe} \langle \text{Tl} \rangle$ sample before and after γ -irradiation differed little. The shape of the experimental curves $\text{tg}\delta(f)$ in the $\text{GaSe} \langle \text{Tl} \rangle$ sample is characteristic of the frequency variation of the dielectric losses, taking into account the contributions of the relaxation mechanism and the electrical conductivity of the crystal [14]. The observation of the maximum on the curve $\text{tg}\delta(f)$ indicates relaxation losses in $\text{GaSe} \langle \text{Tl} \rangle$. The presence of one maximum on the $\text{tg}\delta(f)$ curve indicates that the $\text{GaSe} \langle \text{Tl} \rangle$ single

crystal has one relaxation time. For relaxation processes at the frequency $f = f_i$ [15]

$$\operatorname{tg} \delta_{\max} = \frac{\varepsilon'_{st} - \varepsilon'_{opt}}{2\sqrt{\varepsilon'_{st} \cdot \varepsilon'_{opt}}} \quad (1)$$

Knowing the experimental values of $\operatorname{tg} \delta_{\max}$ and ε'_{opt} from relation (1), the static permittivity (ε'_{st}) of the GaSe <TI> single crystal was calculated (the largest possible value of ε' of the crystal at an infra-low frequency or at a constant voltage). The calculated values of ε'_{st} of the GaSe <TI> sample before and after γ -irradiation are given in the table, which shows that, unlike ε'_{opt} , the value of ε'_{st} decreases after exposure to the sample γ -irradiation.

The values of increment of dielectric permittivity ($\Delta\varepsilon' = \varepsilon'_{st} - \varepsilon'_{opt}$) of the GaSe <TI> sample before and after γ -irradiation are also calculated, which are also given in the table. The experimentally obtained value $f_t = 10^5$ Hz, at which $\operatorname{tg} \delta$ passes through a maximum, made it possible to determine the relaxation frequency (f_r) from the relation

$$f_t = f_r \sqrt{\frac{\varepsilon'_{st}}{\varepsilon'_{opt}}} \quad (2)$$

The values of f_r in the unirradiated and γ -irradiated GaSe <TI> sample with different doses are given in the last column of the table. In this case, the relaxation time in the unirradiated single crystal GaSe <TI> was $\tau = 4.5 \cdot 10^{-5}$ s, and after γ -irradiation with doses of 50 krad and 2.05 Mrad $\tau = 4 \cdot 10^{-5}$ and $3.7 \cdot 10^{-5}$ s, respectively. Those, after γ -irradiation, the relaxation time in the GaSe <TI> sample decreased. Figure 7 shows the frequency dependences of the ac-conductivity (ac-conductivity) of an unirradiated and γ -irradiated GaSe

<TI> single crystal at $T = 300$ K. As the frequency increased from $5 \cdot 10^4$ to $3.5 \cdot 10^7$ Hz, the value of σ_{ac} increased. Gamma irradiation with a dose of 50 krad had no significant effect on the conductivity of the GaSe <TI> single crystal. After γ -irradiation of the GaSe<TI> sample with a dose of 2.05 Mrad, its ac-conductivity decreased (Fig. 7, curve 3).

4. CONCLUSIONS

The calculation of E_g of a GaSe supercell containing Ga vacancy shows that doping increases the value of $E_g = 1.6$ eV. A similar thing also happens when calculating the $\text{Ga}_{16}\text{Se}_{15}$ supercell containing Se vacancy, where $E_g = 1.7$ eV. To correct the underestimated value of E_g , it is necessary to take into account the corresponding corrections and contributions to the calculation of the energy of the system. The calculated distance between atomic nuclei in a 32-atom GaSe supercell is in good agreement with the experimental data. The calculated length of the intralayer chemical bond is $d(\text{Se}_{12}\text{-Ga}_{25}) = 2.466$ Å, $d(\text{Se}_4\text{-Ga}_{17}) = 2.662$ Å. The interlayer bond distance $d(\text{Ga}_{24}\text{-Ga}_{26}) = 2.39$ Å, $d(\text{Se}_{30}\text{-Se}_{12}) = 3.6995$ Å is in good agreement with the experimental data of ε – GaSe: $d(\text{Se-Ga}) = 2.485$ Å, $d(\text{Ga-Ga}) = 2.383$ Å, $d(\text{Se-Se}) = 3.840$ Å.

It has been established that the dielectric coefficients and conductivity of the ε – GaSe < TI > single crystal exhibit frequency dispersion and also decrease under the influence of γ -irradiation. In other words, by changing the frequency of the alternating electric field applied to the GaSe <TI> single crystal, as well as by the action of γ -irradiation, its dielectric coefficients and conductivity can be controlled.

-
- [1] N.C. Fernelius Prog. Cryst. Growth and Charact. 28, 1994, 275-353.
- [2] P.A. Hu, Z.Z. Wen, L.F. Wang, P.H. Tan, K. Xiao. ACS Nano. 6(7), 2012, 5988–5994. <https://doi.org/10.1021/nm300889c>
- [3] Y. Ni, H. Wu, C. Huang, M. Mao, Z. Wang, X. Cheng. Journal of Crystal Growth. 381, 2013, 10- 14.
- [4] T. Wang, J. Li, Q. Zhao, Z. Yin, Y. Zhang, B. Chen, Y. Xie, W. Jie. Materials. 11(2), 2018, 2–9. <https://doi.org/10.3390/ma11020186>.
- [5] S.M. Asadov, S.N. Mustafaeva, K.I. Kelbaliev. Journal of Multidisciplinary Engineering Science Studies (JMESS). 3(8), 2017, 2018-2023.
- [6] S.M. Asadov, S.N. Mustafaeva, A.N. Mammadov. Journal of Thermal Analysis and Calorimetry. 133(2) 2018, 1135–1141. <https://doi.org/10.1007/s10973-018-6967-7>
- [7] S.M. Asadov, S.N. Mustafaeva, V.F. Lukichev, D.T. Guseinov. Russian Microelectronics. 48(4), 2019, 203-207.
- [8] S.M. Asadov, S.N. Mustafaeva, V.F. Lukichev. Russian Microelectronics. 49(6), 2020, 452-465. <https://doi.org/10.1134/S1063739721010042>.
- [9] S.M. Asadov, S.N. Mustafaeva, V.F. Lukichev, K.I. Kelbaliev. Russian Microelectronics. 50(6), 2021, 452-462. <https://doi.org/10.1134/S1063739721060032>.
- [10] S.N. Mustafayeva. Inorganic Materials. 30(5), 1994, 619-621.
- [11] S.N. Mustafaeva, M.M. Asadov, A.A. Ismailov. Inorganic Materials. 47(9), 2011, 1040 – 1043.
- [12] M.M. Asadov, S.N. Mustafaeva, S.S. Guseinova. Physics of the Solid State. 64(1), 2022, 44-57. <https://doi.org/10.21883/FTT.2022.01.51830.182>
- [13] A. Kuhn, A. Chevy, R. Chevalier. Physica Status Solidi (a). 31(2), 1975, 469–475. <https://doi.org/10.1002/pssa.2210310216>
- [14] V.V. Pasynkov. Materials of electronic engineering M.: Higher School (1986) 368 p.
- [15] Physics of dielectrics. Proceedings of 2nd All-Union conf. / Ed. G.I. Scanavy. M.: Publishing House of the Academy of Sciences of the SSR. 1960. 532 p.